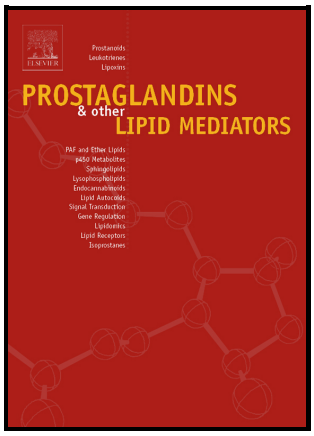

Set up and validation of a sensitive method to quantify prostaglandins, prostaglandin-glycerol esters and prostaglandin-ethanolamides, as well as their respective precursors

Adrien Paquot, Juan Bestard-Escalas, Giulio G. Muccioli

PII: S1098-8823(23)00060-6

DOI: https://doi.org/10.1016/j.prostaglandins.2023.106763

Reference: PRO106763

To appear in: *Prostaglandins and Other Lipid Mediators*

Received date: 4 January 2023
Revised date: 26 May 2023
Accepted date: 27 June 2023

Please cite this article as: Adrien Paquot, Juan Bestard-Escalas and Giulio G. Muccioli, Set up and validation of a sensitive method to quantify prostaglandins, prostaglandin-glycerol esters and prostaglandin-ethanolamides, as well as their respective precursors, *Prostaglandins and Other Lipid Mediators,* (2023) doi:https://doi.org/10.1016/j.prostaglandins.2023.106763

Set up and validation of a sensitive method to quantify prostaglandins, prostaglandin-glycerol esters and prostaglandin-ethanolamides, as well as their respective precursors.

Adrien Paquot[1], Juan Bestard-Escalas[1], Giulio G. Muccioli[1,*]

Bioanalysis and Pharmacology of Bioactive Lipids Research Group, Louvain Drug Research Institute, Université catholique de Louvain, UCLouvain, Av. E. Mounier 72, B1.72.01, B-1200 Bruxelles, Belgium

* Corresponding author:

Giulio G. Muccioli,

giulio.muccioli@uclouvain.be

Bioanalysis and Pharmacology of Bioactive Lipids Research Group (BPBL),

Louvain Drug Research Institute (LDRI),

Université catholique de Louvain (UCL),

Av. E. Mounier, 72 (B1.72.01),

1200 Bruxelles, Belgium

Tel: 0032 2 764 72 31

Abstract

Arachidonic acid-derived prostaglandins are widely studied for their role in inflammation. However, besides arachidonic acid, other arachidonic moiety-containing lipids can be metabolized by COX-2. Indeed, the endocannabinoids 2-arachidonoylglycerol (2-AG) and *N*-arachidonoylethanolamine (anandamide, AEA) can follow the same biochemical pathways than arachidonic acid leading to the formation of prostaglandin-glycerol esters (PG-G) and prostaglandin-ethanolamides (or prostamides, PG-EA), respectively.

The data reported so far support the interest of these bioactive lipids in inflammatory conditions. However, there is only a handful of methods described for their quantification in

biological matrices. Moreover, given the shared biochemical pathways for arachidonic acid, 2-AG and AEA, a method allowing for the quantification of these precursors and the corresponding prostaglandin derivatives appears as largely needed. Thus, we report here the development and validation of a single run UPLC-MS/MS quantification method allowing the quantification of these endocannabinoids-derived mediators together with the classical prostaglandin. Moreover, we applied the method to the quantification of these lipids in vitro (using lipopolysaccharides-activated J774 macrophage cells) and in vivo in several tissues from DSS-induced colitis mice. This femtomole-range method should improve the understanding of the interaction between these lipid mediators and inflammation.

Keywords: PGD_2-G; PGE_2-G; LC-MS; fatty acid; eicosanoid

1. INTRODUCTION

Prostaglandins are well known lipid mediators produced following the metabolism of arachidonic acid by cyclooxygenases (COX, also known as prostaglandin-endoperoxide synthases) followed by specific prostaglandin synthases (**Figure 1**). While arachidonic acid is the prototypical COX-substrate, COX-2 (or PTGS2) is able to use other lipids as substrate, including the endocannabinoids 2-arachidonoylglycerol (2-AG) and anandamide (AEA) [1, 2]. When these two endocannabinoids are the substrates, the PGH_2 derivative resulting from the COX-mediated bis-dioxygenation (i.e. PGH_2-G and PGH_2-EA) is then taken up by prostaglandin synthases to produce the glycerol ester (prostaglandin-glycerol ester, PG-G)

and ethanolamide (prostaglandin-ethanolamide or prostamide, PG-EA) derivatives of PGD_2, PGE_2 and $PGF_{2\alpha}$ [2-4] (**Figure 1**).

It is well established that numerous inflammatory stimuli increase the expression and activity of COX-2 resulting in increased production of prostaglandins (e.g. PGD_2, PGE_2, …) which play a role in controlling inflammation [5-9]. Less is known on the role of the 2-AG derivatives (PG-G) and AEA derivatives (PG-EA) in this context but their study is gaining interest. Reports from our lab and from others point to the biological interest of these lipid mediators [10, 11]. For instance, we have shown that PGD_2-G decreases TLR4-mediated macrophage activation in vitro as well as DSS-induced colitis in vivo [12, 13]. Hu and co-workers showed that intraplantar administration of PGE_2-G induced mechanical allodynia and thermal hyperalgesia [14]. In similar models we have shown that PGD_2-G decreases carrageenan-induced hyperalgesia [11]. Di Marzo's group reported the effects of $PGF_{2\alpha}$-EA on inflammatory pain while Rotondo and co-workers described the effect of PGE_2-EA on monocyte activation [15, 16]. Moreover, Woodward and colleagues put forth the role of prostamide derivatives (e.g. $PGF_{2\alpha}$-EA) in controlling intraocular pressure. These studies resulted in the $PGF_{2\alpha}$-EA analogue Bimatoprost being commercialized for the treatment of glaucoma [17].

While the administration of these molecules (or analogues) or drugs interacting with their metabolism or activity (e.g. COX inhibitors, receptor antagonists) is essential to unravel their biological properties [4, 18-20], a quantification method would bring important complementary information such as the consequences of a given pathophysiological condition on the levels of these lipid mediators. In this line, the quantification of PG and endocannabinoids by HPLC-MS is well established [21-24]. However, only a very limited

number of methods are described to quantify PG-G and PG-EA derivatives. This can be due to the challenges inherent to their quantification, such as their closely related structures (**Figure 1**), and the low levels in biological tissues, especially in uninflamed conditions, for several of these mediators [25].

Gouveia-Figueira et al. reported the quantification of PGE_2-EA in brain tissue from elk, cow and pig using however rather large amounts of tissue (80 mg to 180 mg) when considering the overall lipid content of a brain [26]. We previously detected 15-deoxy$\delta^{12,14}$prostaglandin J_2-glycerol ester (15deoxy$\delta^{12,14}PGJ_2$-G) in the colon of mice using the whole colon (around 200 mg) [13]. More recently, Simone and colleagues used ten mouse dorsal root ganglions to achieve the measurement of PGE_2-G [27]. Finally, Morgan and colleagues detected PG-G in whole mice brain by inhibiting monoacylglycerol lipase (using the inhibitor JZL-184) in mice overexpressing COX-2 [28]. Nevertheless, to our knowledge there is no report of a method allowing the simultaneous quantification of these three families of bioactive lipids and their precursors (i.e. arachidonic acid, 2-AG and AEA).

As an increasing number of reports support the interest of these lipid mediators in pathophysiological situations, we decided to develop a method for the simultaneous extraction, purification, detection, separation and quantification of the PG-G and PG-EA. Moreover, we reasoned that the understanding of the biological phenomena at play would gain from the concomitant quantification of their precursors, namely 2-AG and AEA, as well as from the quantification of the corresponding prostaglandins. Indeed, as we previously reviewed, these biologically relevant lipid mediators share metabolic pathways [4, 20].

Given the low abundance of several of these lipid mediators [20], besides the optimization of the UHPLC-MS/MS method, as for the other methods we developed, we also focused on the

setup of the liquid-liquid extraction and solid-phase extraction (SPE) pre-purification of the analytes [29, 30]. Following the setup of the method and its validation, we demonstrated its applicability to the detection of the lipid of interest using lipopolysaccharides (LPS)-activated J774 cells as well as a mouse model of colitis.

2. MATERIALS AND METHODS

Chemicals

Prostaglandins (prostaglandin D_2 (PGD_2), prostaglandin E_2 (PGE_2), prostaglandin $F_{2\alpha}$ ($PGF_{2\alpha}$), 15-deoxy$\delta^{12,14}$prostaglandin J_2 (15deoxy$\delta^{12,14}$-PGJ_2)), prostaglandin-glycerol esters (prostaglandin D_2-glycerol ester (PGD_2-G), prostaglandin E_2-glycerol ester (PGE_2-G), prostaglandin $F_{2\alpha}$-glycerol ester ($PGF_{2\alpha}$-G), 15-deoxy$\delta^{12,14}$prostaglandin J_2-glycerol ester (15deoxy$\delta^{12,14}$$PGJ_2$-G)), prostaglandin ethanolamides (prostaglandin D_2-ethanolamide (PGD_2-EA), prostaglandin E_2-ethanolamide (PGE_2-EA), prostaglandin $F_{2\alpha}$-ethanolamide ($PGF_{2\alpha}$-EA)), as well as their respective precursors (arachidonic acid, 2-arachidonoylglycerol (2-AG), anandamide (AEA)) were purchased from Sanbio (The Netherlands). Deuterated internal standards (d_8-arachidonic acid, d_5-1-AG, d_4-AEA, d_4-PGE_2, d_5-PGE_2-G and d_4-PGE_2-EA) were also purchased from Sanbio (The Netherlands). HPLC- and MS-grade solvents (chloroform ($CHCl_3$), methanol (MeOH), hexane (Hex), isopropanol (iPOH) and acetonitrile (ACN)) and MS-grade acetic acid were from VWR (Belgium). Butylated hydroxytoluene (BHT), ethylenediaminetetraacetic acid disodium salt dihydrate (EDTA) and LPS (*Escherichia coli*, O55:B5) were from Sigma Aldrich (Belgium). Dextran sodium sulfate (DSS) was purchased from TdB labs (Sweden).

Sample preparation and purification

For tissues, frozen samples were homogenized in $CHCl_3$ (8 mL). Subsequently, MeOH (4 mL, containing 10 µg of BHT), H_2O (2 mL, containing 20 ng of EDTA) and internal standards (d_8-arachidonic acid 15 pmol, d_5-1-AG 15 pmol, d_4-AEA 5 pmol, d_4-PGE_2 15 pmol, d_5-PGE_2-G 5 pmol and d_4-PGE_2-EA 5 pmol/sample, respectively) were added to the vials. For the analysis of the lipids in J774 cell cultures, we prepared a series of vials for the analysis of the cell culture media containing a mixture of $CHCl_3$-MeOH (8:4; v/v) and the internal standards and a series of vials for the analysis of the cells containing $CHCl_3$ and the internal standards. Firstly, media was recovered and transferred to the corresponding vial. Then cells were scraped from the petri dishes with 2 mL PBS (+EDTA) and transferred to the corresponding vial. The petri dishes were then rinsed with 4 mL MeOH (+BHT) that were transferred to the corresponding vial.

Vials were sonicated thoroughly in an ice bath and then centrifuged 10 min at 700*xg* at 4°C. The organic layer was recovered and brought to dryness under a nitrogen stream. Samples were reconstituted in $CHCl_3$-MeOH (99:1; v/v) and transferred on solid phase extraction (SPE) columns packed with silica (SiOH) and conditioned with $CHCl_3$. Loaded SPE were washed with $CHCl_3$ and then the fraction of interest was recovered with 3.5 mL of $CHCl_3$-MeOH (7:3; v/v). The eluent was evaporated under a nitrogen stream and the final purified sample was reconstituted in MeOH (30 µL) for injection.

Lipid analysis by UPLC MS/MS

The reconstituted samples were injected (2 µL) on an acquity UPLC® class H system (Waters) coupled to a Xevo TQ-S mass spectrometer (Waters) used in multiple reaction monitoring (MRM) mode. Mobile phase A consisted in H_2O-ACN-acetic acid (94.9:5:0.1; v/v/v) and mobile phase B in ACN-acetic acid (99.9:0.1; v/v) used in gradient mode. An acquity UPLC®

BEH C18 column from Waters (150x2.1 mm; 1.7 µm) maintained at 40°C was used for lipid separation. Mobile phase gradient was as follows: 80 % of A to 62.5 % of A in 7 min; then 62.5 % to 28.8 % A in 2 min before reaching 95 % B at 17 min; a plateau was maintained during 3 min before re-equilibrating the column. A divert valve was used at the beginning of the run (during 3 min) and at the end of the run (starting at 18 min) to decrease the amount of matrix sent on the mass spectrometer system. Source parameters were designed for PGE_2, PGE_2-G and PGE_2-EA in both positive and negative mode, thus a total of 6 parameter sets. Then the optimal parameters for the mass spectrometer were selected based on the signal to noise ratio obtained after analysis of each of the analytes of interest in the six parameter sets. The selected parameters are as follows: capillary voltage at 3.60 kV; cone voltage at 30 V; desolvation temperature at 550°C; desolvation gas flow at 1000 L/h; cone gas flow at 300 L/h; nebulizer pressure at 7 bar. MRM transitions were then optimized **(supplemental table 1)**. For each molecule, cone voltage was optimized on the quantification transition (Q) and subsequently collision energy was optimized for the three principal MRM transitions on the selected cone voltage value to choose the parameters giving the best detection. Finally, for each compound, two transitions were selected, a quantification (Q) transition used for the calibration curves and a qualification (q) transition to support the nature of the compound detected.

To normalize the data, the ratio between the area under the curve (AUC) of the analyte of interest and the AUC of the respective internal standard was used. To cover the chemical diversity of the molecules of interest we selected six different internal standards (i.e. d_8-arachidonic acid, d_5-1-AG, d_4-AEA, d_4-PGE_2, d_5-PGE_2-G and d_4-PGE_2-EA). When cells were analyzed the data were normalized to the number of cells or the volume of media analyzed.

When tissues were analyzed the data were normalized to the weight (or volume for the plasma) of sample.

Method validation

Specificity

The specificity was evaluated by analyzing several matrices (colon, brain, plasma) with the procedure described above. For each molecule, we selected a quantification transition (Q) and a qualification transition (q) to increase the confidence of the identification.

Trueness

Trueness was evaluated on the three quality control levels of the calibration curves (low, middle and high). Bias was determined on the reference values of the calibration curves and trueness was express in relative bias (%).

Linearity, calibration curves, LOD and LOQ

11 points calibration curves were designed using an evenly-spaced calibration points strategy. The calibration point solutions were prepared in methanol and to ensure that the calibration curves were as close as possible from biological sample analysis, the whole analytical procedure was used to perform the calibration curves. Following the analysis, the ratios between the AUC of the analyte of interest and the AUC of its internal standard were determined and linear regression was selected as mathematical model.

The lower points of the calibration curves were selected as starting points to determine LOD and LOQ by further serial dilution. Thus, for each analyte we prepared 10 serial dilutions and the LOD and LOQ were determined using signal to noise values. Based on FDA [31] and European Pharmacopoeia (Ph. Eur.) [32] guidelines, we compared the signal obtained for a

low concentration sample with the signal obtained at the same retention time in a blank sample analyzed in the same manner. We selected the amount providing at least a signal to noise (S/N) of 3 in nine different replicates obtained from three independent experiment in the case of LOD and one S/N of 10 for the LOQ.

Linearity was controlled regarding the parameters of the linear regression. For each compound, five points covering the entire calibration range were selected and linearity was determined by plotting the ratio obtained by analyzing known amount of the respective five points in the calibration curves. The slope and R square values of the new linear regressions were then used as linearity criteria in accordance with the guidelines.

Intra- and inter-day precision and accuracy

To determine intra- and inter-day precision, we selected, as recommended by the guidelines (i.e. FDA, Ph. Eur.), at least three quality control levels: the LOQ, low, middle and high levels as reported in the **supplemental table 2** [31, 32]. The four levels were analyzed at day one (five replicates per level) and then newly analyzed at day 1, 2 and 3 (three replicates per level) to determine the different precision criteria. The coefficient of variation (CV) was determined for each level and had to be comprise in the ±20 % of confidence interval recommended by the guidelines when considering endogenous compounds or impurities presence in tissue homogenates [33]**.**

Accuracy was determined using the same quality control levels by comparing the bias of each values with the reference ratio of each level. Accuracy values were determined based on three days of analysis. By computing the average values of each level, we determined the accuracy of the method.

Quantification of the lipids of interest in naïve and activated J774 cells

As we previously reported, J774 cells were cultured (37 °C in a humidified 5% CO_2 incubator) in RPMI 1640 medium containing fetal bovine serum (10%) and antibiotics (100 units/mL of penicillin and 100 µg/mL of streptomycin). For the experiments, cells ($18*10^6$ cells/sample) were incubated with LPS (*Escherichia coli*, O55:B5) at 100 ng/mL or vehicle during 24h [12, 34]. After the incubation, cells and the culture media were analyzed separately as described above.

Quantification of the lipids of interest in tissues from control and DSS-induced colitis mice

Colitis was induced in C57BL/6 male mice as we previously reported [13, 35, 36]. To induce colitis, 5% DSS was added to the drinking water during 5 days, and then replaced with normal drinking water for the remaining two days of the protocol. Control mice received normal drinking water during the 7-days protocol. During the experiment body weight was monitored daily. On day 7, mice were anesthetized using isoflurane and blood collected from the cava vein and the portal vein. Mice were then euthanized by cervical dislocation and the tissues removed and snap-frozen in liquid nitrogen before being stored at -80°C. The tissues were processed for lipid quantification as described above. This study was performed in compliance with the European Directive 2010/63/EU, transformed into the Belgian Law of May 29, 2013 regarding the protection of laboratory animals. Lab agreement number LA1230365 and Université catholique de Louvain's animal studies ethics committee approval 2017/UCL/MD/024.

Statistical analysis

Statistical analysis was performed using GraphPad Prism v9.1.2 Software (San Diego, CA). The significance was set at p value < 0.05. For each set of values, normality and variance were controlled. Student t-test (or Mann-Whitney test if distribution was non-parametric)

was used to compare two conditions and ANOVA (or Kruskal-Wallis test if non-parametric) was used to compare three or more conditions. Grubb's test was used to identify potential outliers (when applicable). FDR assessment was based on Benjamini-Hochberg method.

3. RESULTS AND DISCUSSION

3.1 Method development

For the set-up of the extraction and purification procedures, we selected arachidonic acid, 2-AG, AEA, PGD_2, PGD_2-G and PGD_2-EA as representative compounds of their respective families. The mass parameters were determined and the validation was performed for the whole set of analytes of interest. Of note, while 2-AG is considered the most relevant isoform of arachidonoylglycerol, it is largely descried that 2-AG undergo fast interconversion into the more stable 1(3)-AG depending on the experimental conditions. Thus, most developed methods report 2-AG levels by considering the chromatographic peak of 2-AG and 1(3)-AG. Therefore, even if the chromatographic system we use resolved the two isomers, we followed a similar strategy for our method and quantified 2-AG as the signal from 2-AG and 1(3)-AG.

Optimization of the MS/MS detection and of the separation of the derivatives

We prepared standard solutions for each compound at 10^{-5} M in ACN-H_2O (1:1; v/v) to start the optimization process of the parameters of the tandem quadrupole mass spectrometer. This step allowed us to define MRM transitions as well as mass spectrometer parameters to use for each compound. Following Intellistart® (Waters)-guided design of transitions performed in positive and negative ionization mode, we fine-tuned the selection of the

MRM transitions by implementing several transitions published in the literature [26, 37, 38], as well as additional potential transitions based on the structure of the compounds.

In parallel to the selection of the MRM transitions, we optimized the parameters of the mass spectrometer for the detection of the analytes of interest. For this we tuned one prostaglandin (PGE_2), one PG-G (PGE_2-G) and one prostamide (PGE_2-EA) in positive and negative modes. Then, we analyzed an equimolar mixture of all the standards in the 6 different mass parameters. Of note, in our working conditions, we did not find any satisfying MRM transition for AEA, 2-AG and $PGF_{2\alpha}$-G in negative mode. As reported in **supplemental Figure 1**, the positive mode seems superior to the negative mode for our analytes of interest. Based on the data obtained, we selected the tune parameters obtained for PGE_2-G (in positive mode) as this gives us the best compromise when considering the whole set of analytes. Once the quantification and qualification transitions selected for each derivative (**Table 1**), we optimized the separation by testing several mobile phase compositions and gradients (**data not shown**) using two different UHPLC columns (the Kinetex® EVO C18 (100x2.1 mm; 1.7 µm) and the Waters acquity UPLC® BEH C18 (150x2.1 mm; 1.7 µm) columns) previously described in the literature to resolve several prostaglandin derivatives [26, 39, 40]. In our hands, when compared with the EVO C18 column, used in the same chromatographic conditions, the BEH column resulted in larger width and decreased intensity for the peak of 2-AG and others precursors. However, the opposite was observed for the peaks of PG-G and PG-EA (which are reported as less abundant in biological samples) (**Supplemental Figure 2A**). Moreover, when assessing chromatographic peak shape, the BEH column allows to separate the family isomers (e.g. PGD_2-G and PGE_2-G) but also the position isomers of the prostaglandin glycerol ester series (e.g. PGD_2-1-G and PGD_2-2-G) when compared to the EVO C18 column (**Supplemental Figure 2B**). Based on these elements we

selected the acquity BEH C18 column for our method. The resulting chromatographic method allows us to analyze the complete set of analytes within 15 min of run (**Figure 2**).

Optimization of the parameters of the tandem quadrupole

As discussed above, we used the automatic Intellistart® module provided by the MassLynx® software to tune the molecules both in positive and negative ionization modes (**supplemental Figure 1**). Besides this initial set up, several others parameters can also be optimized to increase the detection of the analytes. First, with an incremental strategy, we decided to assess the source height, inclination, desolvation gas flow and cone gas flow together (**data not shown**). This led to an overall improvement of the detection of the analytes (spiked in a biological matrix) of 10-30% (**supplemental Figure 3A**). We then assessed the influence of the cone voltage on the detection of the analytes of interest using the quantification MRM transition (**supplemental Table 1 and Figure 3B**). Based on the obtained data we selected a cone voltage value of 30 volts. Next, we assessed the effect of the collision energy (CE) on the signal obtained for the three selected transitions for each lipid. By varying the CE between 2 eV and 50 eV we selected for each of the 14 lipids of interest the most appropriate CE and transition (**Figure 3 and supplemental Table 1**).

Optimization of the extraction procedure

Besides the MS parameters, quantitative analysis of low-abundance lipids in complex matrices requires a careful assessment of the extraction and purification procedures. Thus, based on previous protocols used in our lab [29, 30], we optimized the extraction and purification procedures. As with many methods for lipid analysis, we decided to use a Folch-type liquid-liquid extraction to obtain an efficient extraction from biological matrices [41]. While the original method used $CHCl_3$, we first decided to assess if replacing it with the less

harmful dichloromethane (CH_2Cl_2) would be feasible (i.e. would not affect extraction yield). As reported in **supplemental Figure 4**, the extraction of the analytes in the presence of CH_2Cl_2 is significantly less efficient than in the presence of $CHCl_3$.

Although the chemical structures of the prostaglandin derivatives we are interested in are quite similar, the three families differ by the polar head (i.e. prostaglandins have an ionizable carboxylic group whereas PG-EA and PG-G have a small non-ionizable polar moiety) (**Figure 1**). Thus, we decided to assess whether acidification of the extraction mixture, composed of $CHCl_3$, MeOH and H_2O, would improve the extraction yield of the prostaglandins (due to the presence of a carboxylic moiety). In the presence of standards only, the acidification resulted in a slight decrease in 2-AG and PGD_2-EA signal, but did not improve the signal for arachidonic acid or PGD_2 (**Figure 4A**). Strikingly, the acidification appeared as highly deleterious for the detection of most derivatives when assessed in the presence of a biological matrix (**Figure 4B**). Indeed, except for arachidonic acid, acidification decreased the detection of all the lipid of interest when extracted from the matrix. When comparing the data obtained in the absence and presence of matrix, one can speculate that the decreased signal is in part due to a higher extraction of other molecules present in the matrix [29, 42, 43]. Typically, phospholipids are known to be better extracted in acidic condition and to affect MS detection by ion-suppression effects [44].

The next step of the analytical method is a silica-based SPE purification procedure. This requires to select appropriate washing and elution steps. Thus, we looked for a solvent that would elute the more lipophilic compounds present in a biological matrix (typically cholesterol) while retaining the lipid mediators of interest on the column. Based on a previously validated method from our laboratory, we tested $CHCl_3$ (2 and 4 ml) as washing

solvent [30]. As shown in **Figure 5A**, this resulted in the complete elution of cholesterol while retaining the lipids of interest on the column. Then we tested several solvent mixtures to determine the best eluent to recover the compounds of interest from the SPE. Based on preliminary data, we tested several mixtures of chloroform and methanol containing increasing proportions of methanol. This led to the selection of $CHCl_3$-MeOH (7:3; v/v) to effectively recover the analytes of interest (**Figure 5B**). Indeed, higher proportions of methanol would result in higher levels of phospholipids in the sample resulting in unnecessary matrix effects [29]. Of note, we decided to use 30% of methanol as lower methanol content yielded more variable results during the numerous assay we performed during the method development.

3.2 Method validation

Specificity and selectivity

The selectivity is a critical parameter when analyzing prostaglandins as some of them are isomers of each other. Moreover, the glycerol ester series present a chromatographic double peak due to the interconversion of the glycerol position on the acyl chain (also identified with the 2-AG [45]). This was improved by selecting the best separation parameters after testing several UPLC columns as well as several mobile phases and gradients (data not shown). As mentioned above, an acquity UPLC® BEH C18 column from Waters (150x2.1 mm; 1.7 µm) was selected together with a gradient of H_2O-ACN-acetic acid (94.9:5:0.1; v/v/v) and ACN-acetic acid (99.9:0.1; v/v).

To go further we selected three representative matrices in term of lipid content (i.e. colon, brain and plasma) to examine whether the matrix content could affect compounds detection (e.g. coelution with others endogenous compounds or signal modification) or compounds

separation (e.g. decrease in the resolution of peaks). For that, we applied the complete procedure to analyze the matrix alone, the standards alone and the matrix spiked with the standards. As illustrated in **supplemental Figure 5**, with PGE_2-G and $PGF_{2\alpha}$-EA used as example, none of the three selected matrices affects neither the detection nor the chromatographic separation of the analytes (as shown here for PGE_2-G). Validation of quantification methods for endogenous compounds is made more complex by the absence of biological blank matrix (i.e. tissue or cells not containing the analytes of interest). Thus, to assess how the matrix would affect the detection of the analytes, we compared the signal obtained in the absence or in the presence of matrix (colon, brain, plasma) for the 6 deuterated standards used in the method (**Supplemental Figure 6**). For most of the conditions the signal of the deuterated standard was not altered by the presence of matrix. In the presence of colon, the signal of d_4-AEA was increased while the signal of d_4-PGE_2 was decreased. In the presence of brain as matrix, only the signal of d_8-AA was decreased compared to the signal obtained in the absence of matrix.

Calibration curves and response function

Based on the literature and on previous works of our research group, we expected the endogenous levels of PG-EA and PG-G to be low and likely near the instrument limits of detection. On the contrary, the endogenous levels of arachidonic acid and 2-AG are quite high in comparison with the PG-G and PG-EA. Based on the information gathered during the method development, we selected 900 fmol on column as the highest point of the calibration curve for the majority of the compounds. For arachidonic acid and 2-AG (9000 fmol on column) and for 15deoxy$\delta^{12,14}PGJ_2$ (1800 fmol on column) higher amounts were selected. To avoid leverage effect, we opted for the use of an evenly-spaced calibration

points strategy and designed 11 points calibration curves. The lowest point of the calibration curve was 40 fmol on column, except for 15deoxy$\delta^{12,14}PGJ_2$ (80 fmol on column) and arachidonic acid as well as 2-AG (400 fmol on column). To consider the whole analytical process used for analyzing biological samples, the solutions prepared for the calibration curves were analyzed by using the whole analytical process (i.e. extraction, SPE purification and LC-MS analysis).

To ensure the best fit between the experimental points and the calibration curve, several models were tested and the goodness of fit assessed [46]. Considering a 25% confidence interval between each value and the mathematical regression, a linear regression was selected (**Table 2**). This confidence interval was chosen as we are developing a quantification method for measuring endogenous compounds in biological matrices [33].

Trueness

Trueness was evaluated on three quality control levels based on the calibration curves (i.e. low, middle and high) (**supplemental table 2**). The relative bias of each level was determined and all the values were found to be within the 20 % of acceptance criteria (**Table 2**). The highest value was observed for the lowest level of PGD_2 where -17,34 % of relative bias was obtained.

Limits of detection and quantification

Starting from the lowest point of the calibration curves, we prepared 10 serial dilutions to determine the LOD and LOQ of the method based on signal to noise values. We performed three experiments (in triplicate) and the LOD was determined as the amount giving a signal to noise of 3 for the nine replicates and the LOQ was the amount giving a signal to noise of 10 for the nine replicates (**table 2**). When comparing the effect of the “polar head”, it

appears that our method is more sensitive for the ethanolamide derivatives (PG-EA and AEA) when compared with the glycerol derivatives (PG-G, 2-AG) and with the carboxylic acid derivatives (PG and arachidonic acid). When comparing the prostaglandin series analyzed here, it seems that the method is slightly more sensitive for the detection of the $F_{2\alpha}$ moiety compared to the D_2 and E_2 series.

Intra- and interday precision and accuracy

Based on the calibration curves, we selected four quality control levels to assess the precision criteria of the method (**supplemental table 2**). After determining the variation coefficient for the different precision levels, we assessed whether the values were comprised inside the confidence values of ± 15 % according with the guidelines [31, 47] (**Table 2**). For both repeatability and intermediate precision, the determined values obtained were comprised in the confidence intervals allowed by the guidelines.

We used the same quality control levels, injected at least at three different time points, to determine the accuracy (bias) inherent to the method (**Table 2**). The method provided good accuracy values. Of note, we obtained for $PGF_{2\alpha}$-EA at the LOQ level a value of 15.3 % which is still acceptable when considering the fact that for low quality control level a confidence interval of 20 % is allowed.

3.3 Quantification of the prostaglandin derivatives in the J774 macrophage cell line

To test the applicability of our method, we decided to assess, in J774 cells, the effect of a pro-inflammatory stimulus on the levels of the PG, PG-G and PG-EA derivatives. J774 cells is a macrophage cell line largely used when studying lipid mediators in the context of inflammation. As we and others have shown, incubation of the cells with LPS results in the production of pro-inflammatory mediators (e.g. IL-6, TNFα, MCP-1) and the overexpression

of several enzymes involved in inflammation, including COX-2 [12, 34, 48]. As we have previously used this cell line to study the anti-inflammatory mechanism of PGD_2-G [12], we thought it would be an interesting model to test our method.

Although we were not able to detect all the lipid mediators in the vehicle-treated condition (i.e. control condition), following incubation of the cells with LPS our method allowed us to quantify several of the lipid mediators of interest (**Figure 6**). As expected, prostaglandins are much more abundant than the corresponding PG-G, which in turn are more abundant than the PG-EA. Incubation of the cells with LPS resulted in decreased cell levels of arachidonic acid and increased cell levels of the prostaglandins. This increase was also apparent in the cell culture medium. For the endocannabinoid 2-AG we observed a similar trend with decreased cell levels of 2-AG and increased cell levels of PG-G. For AEA we observed a different trend as cell incubation with LPS resulted in increased levels of the endocannabinoid, as we previously reported [34]. As for the PG-EA we observed a strong increase in their levels in the cell incubation media, but no detection (except for PGD_2-EA) in the cells.

Prostaglandins are described as secreted mediators, detecting them in the cell culture media in larger amounts than in the corresponding cell samples is therefore not surprising [49]. Less is known on the secretion of PG-G and PG-EA, however their presence in the cell culture media is coherent with the fact that they can act as biological mediators.

3.3 Quantification of the prostaglandin derivatives in a DSS-induced colitis mouse model

To test further the applicability of our method, we decided to assess the effect of a DSS-induced colitis (**supplemental Figure 7**) on the levels of the lipid mediators of interest in several tissues of relevance in the context of colitis. We chose this model as we have

previously shown that administering or altering endocannabinoid and PG-G derivative levels can decrease colitis extent [13, 36, 50]. Moreover, our and other works have shown that the levels of these lipid mediators are altered in the context of colon inflammation [13, 36, 50-53]. In this study, besides the colon, we also analyzed the draining lymph nodes as well as the spleen that are important tissues in the immune response involved in the disease. Also, we analyzed the visceral adipose tissue as it has also been shown to be subjected to inflammation during colitis [54-56]. Finally, we also measured the lipid levels in the blood from the portal and the cava veins, as well as the liver (**Supplemental table 3**).

As shown in **Figure 7**, in accordance with the literature [53], we observed an overall increase in prostaglandin levels due to colitis induction (the tissue levels are reported in **Supplemental table 3**). In the plasma, we observed that while PGE_2 levels increased in portal vein, they were decreased in the cava vein. Regarding the PG-G, only PGE_2-G was present in levels high enough to be quantified (i.e. above the LOQ of the method). Its levels were decreased in the colon and increased in the visceral adipose tissue due to the DSS-induced colitis. However, colitis did not change PGE_2-G levels in the lymph nodes and spleen. Unfortunately, we were unable to detect prostamide derivatives in the analyzed tissues. The fact that AEA levels are much lower than 2-AG levels could explain the much lower levels of PG-EA which are below the LOD of our method. This is supported by our in vitro data as we found lower levels of PG-EA compared to PG-G levels. At the biological level we found quite marked variations in lipid levels in the visceral adipose tissue further supporting its sensitivity to colon inflammation. Further quantifications of bioactive lipids in this tissue are warranted in both preclinical and clinical studies on colitis.

4. Conclusion

As mentioned, low endogenous abundance represents the main challenge when quantifying in biological matrices PG-EA, and to a lesser extent PG-G, derivatives. In this report we described an UHPLC-MS/MS method allowing the single-run quantification of prostaglandins and their glycerol ester and ethanolamide analogues, as well as their respective biochemical precursors. The use of this femtomole-range method will improve our understanding of the interactions between these lipid mediators that share biochemical pathways and receptors.

Acknowledgements

G.G. Muccioli is the recipient of subsidies from the Fonds Spéciaux de Recherches (FSR, Université catholique de Louvain) and from the FRS-FNRS, Belgium. The MASSMET platform is acknowledged for the access to the mass spectrometer. Prof. Mireille Alhouayek (LDRI, UCLouvain) is acknowledged for her expertise and help with the colitis model.

Authors contribution

A. Paquot and G. G. Muccioli designed the research; A. Paquot performed experiments and analyzed the data; J. Bestard-Escalas conducted the in vitro experiments; A. Paquot and G. G. Muccioli wrote the manuscript; G.G. Muccioli supervised the whole study; and all authors read and approved the manuscript.

Conflicts of interest

The authors declare that they have no competing interests

[1] K.R. Kozak, S.W. Rowlinson, L.J. Marnett, Oxygenation of the endocannabinoid, 2-arachidonylglycerol, to glyceryl prostaglandins by cyclooxygenase-2, J Biol Chem 275(43) (2000) 33744-9.
[2] M. Yu, D. Ives, C.S. Ramesha, Synthesis of prostaglandin E2 ethanolamide from anandamide by cyclooxygenase-2, J Biol Chem 272(34) (1997) 21181-6.
[3] K.R. Kozak, J.J. Prusakiewicz, S.W. Rowlinson, C. Schneider, L.J. Marnett, Amino acid determinants in cyclooxygenase-2 oxygenation of the endocannabinoid 2-arachidonylglycerol, J Biol Chem 276(32) (2001) 30072-7.
[4] M. Alhouayek, G.G. Muccioli, COX-2-derived endocannabinoid metabolites as novel inflammatory mediators, Trends Pharmacol Sci 35(6) (2014) 284-92.
[5] C. Yao, S. Narumiya, Prostaglandin-cytokine crosstalk in chronic inflammation, Br J Pharmacol 176(3) (2019) 337-354.
[6] T. Schmid, B. Brune, Prostanoids and Resolution of Inflammation - Beyond the Lipid-Mediator Class Switch, Front Immunol 12 (2021) 714042.
[7] O.O. Oyesola, E.D. Tait Wojno, Prostaglandin regulation of type 2 inflammation: From basic biology to therapeutic interventions, Eur J Immunol 51(10) (2021) 2399-2416.
[8] R. Rajakariar, M.M. Yaqoob, D.W. Gilroy, COX-2 in inflammation and resolution, Mol Interv 6(4) (2006) 199-207.
[9] E. Ricciotti, G.A. FitzGerald, Prostaglandins and inflammation, Arterioscler Thromb Vasc Biol 31(5) (2011) 986-1000.
[10] B. Buisseret, O. Guillemot-Legris, Y. Ben Kouidar, A. Paquot, G.G. Muccioli, M. Alhouayek, Effects of R-flurbiprofen and the oxygenated metabolites of endocannabinoids in inflammatory pain mice models, FASEB J 35(4) (2021) e21411.
[11] B. Buisseret, O. Guillemot-Legris, G.G. Muccioli, M. Alhouayek, Prostaglandin D2-glycerol ester decreases carrageenan-induced inflammation and hyperalgesia in mice, Biochim Biophys Acta Mol Cell Biol Lipids 1864(5) (2019) 609-618.
[12] M. Alhouayek, J. Masquelier, P.D. Cani, D.M. Lambert, G.G. Muccioli, Implication of the anti-inflammatory bioactive lipid prostaglandin D2-glycerol ester in the control of macrophage activation and inflammation by ABHD6, Proc Natl Acad Sci U S A 110(43) (2013) 17558-63.
[13] M. Alhouayek, B. Buisseret, A. Paquot, O. Guillemot-Legris, G.G. Muccioli, The endogenous bioactive lipid prostaglandin D2-glycerol ester reduces murine colitis via DP1 and PPARgamma receptors, FASEB J 32(9) (2018) 5000-5011.
[14] S.S. Hu, H.B. Bradshaw, J.S. Chen, B. Tan, J.M. Walker, Prostaglandin E2 glycerol ester, an endogenous COX-2 metabolite of 2-arachidonoylglycerol, induces hyperalgesia and modulates NFkappaB activity, Br J Pharmacol 153(7) (2008) 1538-49.
[15] L. Gatta, F. Piscitelli, C. Giordano, S. Boccella, A. Lichtman, S. Maione, V. Di Marzo, Discovery of prostamide F2alpha and its role in inflammatory pain and dorsal horn nociceptive neuron hyperexcitability, PLoS One 7(2) (2012) e31111.
[16] K.L. Brown, J. Davidson, D. Rotondo, Characterisation of the prostaglandin E2-ethanolamide suppression of tumour necrosis factor-alpha production in human monocytic cells, Biochim Biophys Acta 1831(6) (2013) 1098-107.
[17] D.F. Woodward, A.H. Krauss, J. Chen, Y. Liang, C. Li, C.E. Protzman, A. Bogardus, R. Chen, K.M. Kedzie, H.A. Krauss, D.W. Gil, A. Kharlamb, L.A. Wheeler, D. Babusis, D. Welty, D.D. Tang-Liu, M. Cherukury, S.W. Andrews, R.M. Burk, M.E. Garst, Pharmacological characterization of a novel antiglaucoma agent, Bimatoprost (AGN 192024), J Pharmacol Exp Ther 305(2) (2003) 772-85.
[18] C. Turcotte, F. Chouinard, J.S. Lefebvre, N. Flamand, Regulation of inflammation by cannabinoids, the endocannabinoids 2-arachidonoyl-glycerol and arachidonoyl-ethanolamide, and their metabolites, J Leukoc Biol 97(6) (2015) 1049-70.
[19] R.L. Jones, M.A. Giembycz, D.F. Woodward, Prostanoid receptor antagonists: development strategies and therapeutic applications, Br J Pharmacol 158(1) (2009) 104-45.

[20] B. Buisseret, M. Alhouayek, O. Guillemot-Legris, G.G. Muccioli, Endocannabinoid and Prostanoid Crosstalk in Pain, Trends Mol Med 25(10) (2019) 882-896.
[21] D. Tsikas, A.A. Zoerner, Analysis of eicosanoids by LC-MS/MS and GC-MS/MS: a historical retrospect and a discussion, J Chromatogr B Analyt Technol Biomed Life Sci 964 (2014) 79-88.
[22] L.A. Gobo, L.M. de Carvalho, F. Temp, C. Viana, C.F. Mello, A rapid method for identification and quantification of prostaglandins in cerebral tissues by UHPLC-ESI-MS/MS for the lipidomic in vivo studies, Anal Biochem 545 (2018) 98-103.
[23] W. Rohrig, S. Achenbach, B. Deutsch, M. Pischetsrieder, Quantification of 24 circulating endocannabinoids, endocannabinoid-related compounds, and their phospholipid precursors in human plasma by UHPLC-MS/MS, J Lipid Res 60(8) (2019) 1475-1488.
[24] M.S. Gachet, P. Rhyn, O.G. Bosch, B.B. Quednow, J. Gertsch, A quantitiative LC-MS/MS method for the measurement of arachidonic acid, prostanoids, endocannabinoids, N-acylethanolamines and steroids in human plasma, J Chromatogr B Analyt Technol Biomed Life Sci 976-977 (2015) 6-18.
[25] P. Urquhart, J. Wang, D.F. Woodward, A. Nicolaou, Identification of prostamides, fatty acyl ethanolamines, and their biosynthetic precursors in rabbit cornea, J Lipid Res 56(8) (2015) 1419-33.
[26] S. Gouveia-Figueira, M.L. Nording, Validation of a tandem mass spectrometry method using combined extraction of 37 oxylipins and 14 endocannabinoid-related compounds including prostamides from biological matrices, Prostaglandins Other Lipid Mediat 121(Pt A) (2015) 110-21.
[27] I.A. Khasabova, M. Uhelski, S.G. Khasabov, K. Gupta, V.S. Seybold, D.A. Simone, Sensitization of nociceptors by prostaglandin E2-glycerol contributes to hyperalgesia in mice with sickle cell disease, Blood 133(18) (2019) 1989-1998.
[28] A.J. Morgan, P.J. Kingsley, M.M. Mitchener, M. Altemus, T.A. Patrick, A.D. Gaulden, L.J. Marnett, S. Patel, Detection of Cyclooxygenase-2-Derived Oxygenation Products of the Endogenous Cannabinoid 2-Arachidonoylglycerol in Mouse Brain, ACS Chem Neurosci 9(7) (2018) 1552-1559.
[29] J. Masquelier, G.G. Muccioli, Development and validation of a specific and sensitive HPLC-ESI-MS method for quantification of lysophosphatidylinositols and evaluation of their levels in mice tissues, J Pharm Biomed Anal 126 (2016) 132-40.
[30] V. Mutemberezi, J. Masquelier, O. Guillemot-Legris, G.G. Muccioli, Development and validation of an HPLC-MS method for the simultaneous quantification of key oxysterols, endocannabinoids, and ceramides: variations in metabolic syndrome, Anal Bioanal Chem 408(3) (2016) 733-45.
[31] Q2(R1) Validation of Analytical Procedures: Text and Methodology Guidance for Industry, 2021. https://www.fda.gov/regulatory-information/search-fda-guidance-documents/q2r1-validation-analytical-procedures-text-and-methodology-guidance-industry.
[32] European Pharmacopoeia (Ph. Eur.) 10th Edition l EDQM - European Directorate for the Quality of Medicines. https://www.edqm.eu/en/european-pharmacopoeia-ph.-eur.-11th-edition.
[33] P. Timmerman, S. White, S. McDougall, M.A. Kall, J. Smeraglia, M.S. Fjording, M. Knutsson, Tiered approach into practice: scientific validation for chromatography-based assays in early development - a recommendation from the European Bioanalysis Forum, Bioanalysis 7(18) (2015) 2387-2398.
[34] M. Alhouayek, P. Bottemanne, A. Makriyannis, G.G. Muccioli, N-acylethanolamine-hydrolyzing acid amidase and fatty acid amide hydrolase inhibition differentially affect N-acylethanolamine levels and macrophage activation, Biochim Biophys Acta Mol Cell Biol Lipids 1862(5) (2017) 474-484.
[35] O. Guillemot-Legris, V. Mutemberezi, B. Buisseret, A. Paquot, V. Palmieri, P. Bottemanne, J. Lemaire, J.F. Rahier, M. Alhouayek, G.G. Muccioli, Colitis Alters Oxysterol Metabolism and is Affected by 4beta-Hydroxycholesterol Administration, J Crohns Colitis 13(2) (2019) 218-229.
[36] M. Alhouayek, P. Bottemanne, K.V. Subramanian, D.M. Lambert, A. Makriyannis, P.D. Cani, G.G. Muccioli, N-Acylethanolamine-hydrolyzing acid amidase inhibition increases colon N-palmitoylethanolamine levels and counteracts murine colitis, FASEB J 29(2) (2015) 650-61.
[37] G. Dasilva, S. Munoz, S. Lois, I. Medina, Non-Targeted LC-MS/MS Assay for Screening Over 100 Lipid Mediators from ARA, EPA, and DHA in Biological Samples Based on Mass Spectral Fragmentations, Molecules 24(12) (2019).

[38] L. Kiss, Y. Roder, J. Bier, N. Weissmann, W. Seeger, F. Grimminger, Direct eicosanoid profiling of the hypoxic lung by comprehensive analysis via capillary liquid chromatography with dual online photodiode-array and tandem mass-spectrometric detection, Anal Bioanal Chem 390(2) (2008) 697-714.
[39] F. Fanti, F. Vincenti, C. Montesano, M. Serafini, D. Compagnone, M. Sergi, dLLME-muSPE extraction coupled to HPLC-ESI-MS/MS for the determination of F2alpha-IsoPs in human urine, J Pharm Biomed Anal 186 (2020) 113302.
[40] Y. Yang, Q. Zhong, C. Mo, H. Zhang, T. Zhou, W. Tan, Determination of endogenous inflammation-related lipid mediators in ischemic stroke rats using background subtracting calibration curves by liquid chromatography-tandem mass spectrometry, Anal Bioanal Chem 409(28) (2017) 6537-6547.
[41] J. Folch, I. Ascoli, M. Lees, J.A. Meath, B.N. Le, Preparation of lipide extracts from brain tissue, J Biol Chem 191(2) (1951) 833-41.
[42] X. Bai, F.G. Naghdi, L. Ye, P. Lant, S. Pratt, Enhanced lipid extraction from algae using free nitrous acid pretreatment, Bioresour Technol 159 (2014) 36-40.
[43] S. Pati, B. Nie, R.D. Arnold, B.S. Cummings, Extraction, chromatographic and mass spectrometric methods for lipid analysis, Biomed Chromatogr 30(5) (2016) 695-709.
[44] M. Wilm, Principles of electrospray ionization, Mol Cell Proteomics (2011).
[45] A.A. Zoerner, S. Batkai, M.T. Suchy, F.M. Gutzki, S. Engeli, J. Jordan, D. Tsikas, Simultaneous UPLC-MS/MS quantification of the endocannabinoids 2-arachidonoyl glycerol (2AG), 1-arachidonoyl glycerol (1AG), and anandamide in human plasma: minimization of matrix-effects, 2AG/1AG isomerization and degradation by toluene solvent extraction, J Chromatogr B Analyt Technol Biomed Life Sci 883-884 (2012) 161-71.
[46] E. Rozet, C. Hubert, A. Ceccato, W. Dewe, E. Ziemons, F. Moonen, K. Michail, R. Wintersteiger, B. Streel, B. Boulanger, P. Hubert, Using tolerance intervals in pre-study validation of analytical methods to predict in-study results. The fit-for-future-purpose concept, J Chromatogr A 1158(1-2) (2007) 126-37.
[47] S. Bansal, A. DeStefano, Key elements of bioanalytical method validation for small molecules, AAPS J 9(1) (2007) E109-14.
[48] H. Abdul Khaliq, S. Ortiz, M. Alhouayek, G.G. Muccioli, J. Quetin-Leclercq, Dereplication and Quantification of Major Compounds of Convolvulus arvensis L. Extracts and Assessment of Their Effect on LPS-Activated J774 Macrophages, Molecules 27(3) (2022).
[49] C.D. Funk, Prostaglandins and leukotrienes: advances in eicosanoid biology, Science 294(5548) (2001) 1871-5.
[50] M. Alhouayek, D.M. Lambert, N.M. Delzenne, P.D. Cani, G.G. Muccioli, Increasing endogenous 2-arachidonoylglycerol levels counteracts colitis and related systemic inflammation, FASEB J 25(8) (2011) 2711-21.
[51] S. Melgar, M. Drmotova, E. Rehnstrom, L. Jansson, E. Michaelsson, Local production of chemokines and prostaglandin E2 in the acute, chronic and recovery phase of murine experimental colitis, Cytokine 35(5-6) (2006) 275-83.
[52] K. Lauritsen, L.S. Laursen, K. Bukhave, J. Rask-Madsen, In vivo profiles of eicosanoids in ulcerative colitis, Crohn's colitis, and Clostridium difficile colitis, Gastroenterology 95(1) (1988) 11-7.
[53] J. Kikut, M. Mokrzycka, A. Drozd, U. Grzybowska-Chlebowczyk, M. Zietek, M. Szczuko, Involvement of Proinflammatory Arachidonic Acid (ARA) Derivatives in Crohn's Disease (CD) and Ulcerative Colitis (UC), J Clin Med 11(7) (2022).
[54] A. Zulian, R. Cancello, C. Ruocco, D. Gentilini, A.M. Di Blasio, P. Danelli, G. Micheletto, E. Cesana, C. Invitti, Differences in visceral fat and fat bacterial colonization between ulcerative colitis and Crohn's disease. An in vivo and in vitro study, PLoS One 8(10) (2013) e78495.
[55] P. Desreumaux, O. Ernst, K. Geboes, L. Gambiez, D. Berrebi, H. Muller-Alouf, S. Hafraoui, D. Emilie, N. Ectors, M. Peuchmaur, A. Cortot, M. Capron, J. Auwerx, J.F. Colombel, Inflammatory alterations in mesenteric adipose tissue in Crohn's disease, Gastroenterology 117(1) (1999) 73-81.

[56] E.D. Rivera, J.C. Coffey, D. Walsh, E.D. Ehrenpreis, The Mesentery, Systemic Inflammation, and Crohn's Disease, Inflamm Bowel Dis 25(2) (2019) 226-234.

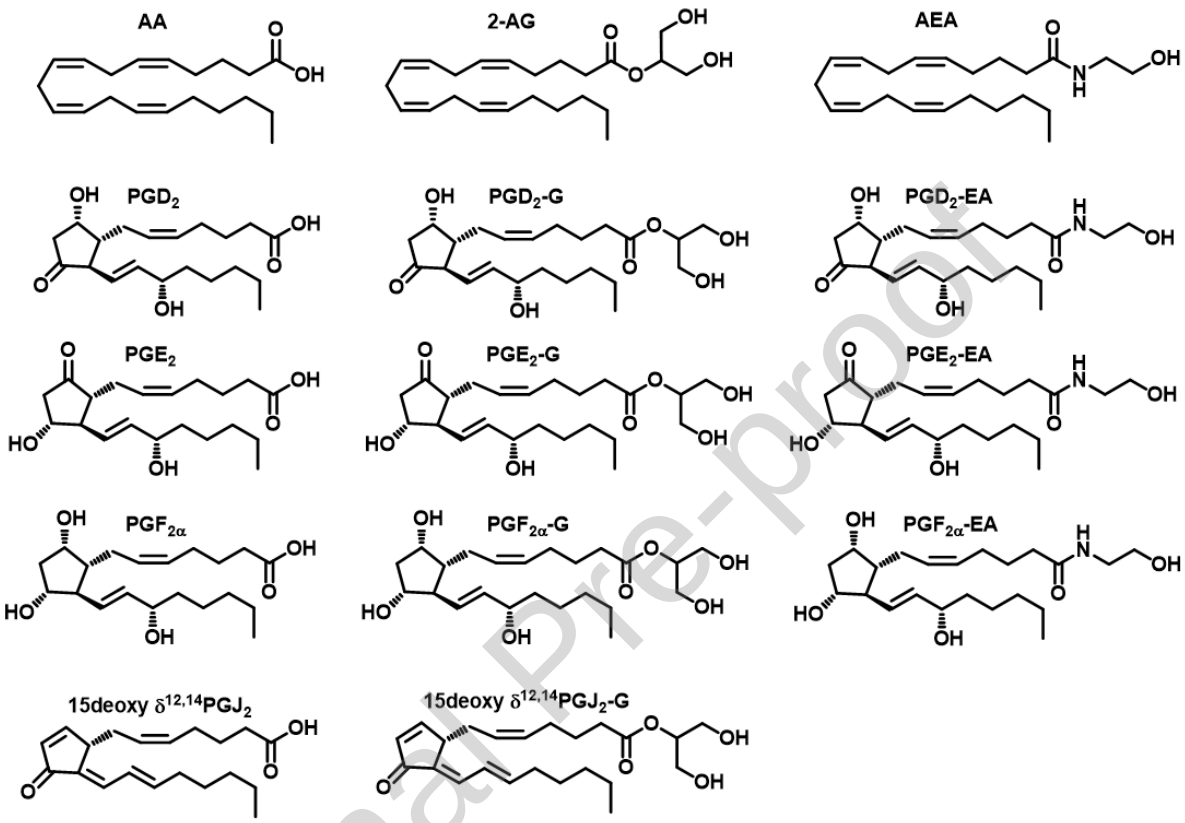

Figure 1: Chemical structure of the lipid mediators quantified by the validated method. Chemical structure of the prostaglandins, prostaglandin-glycerol esters, prostaglandin ethanolamides as well as their respective precursors (top row).

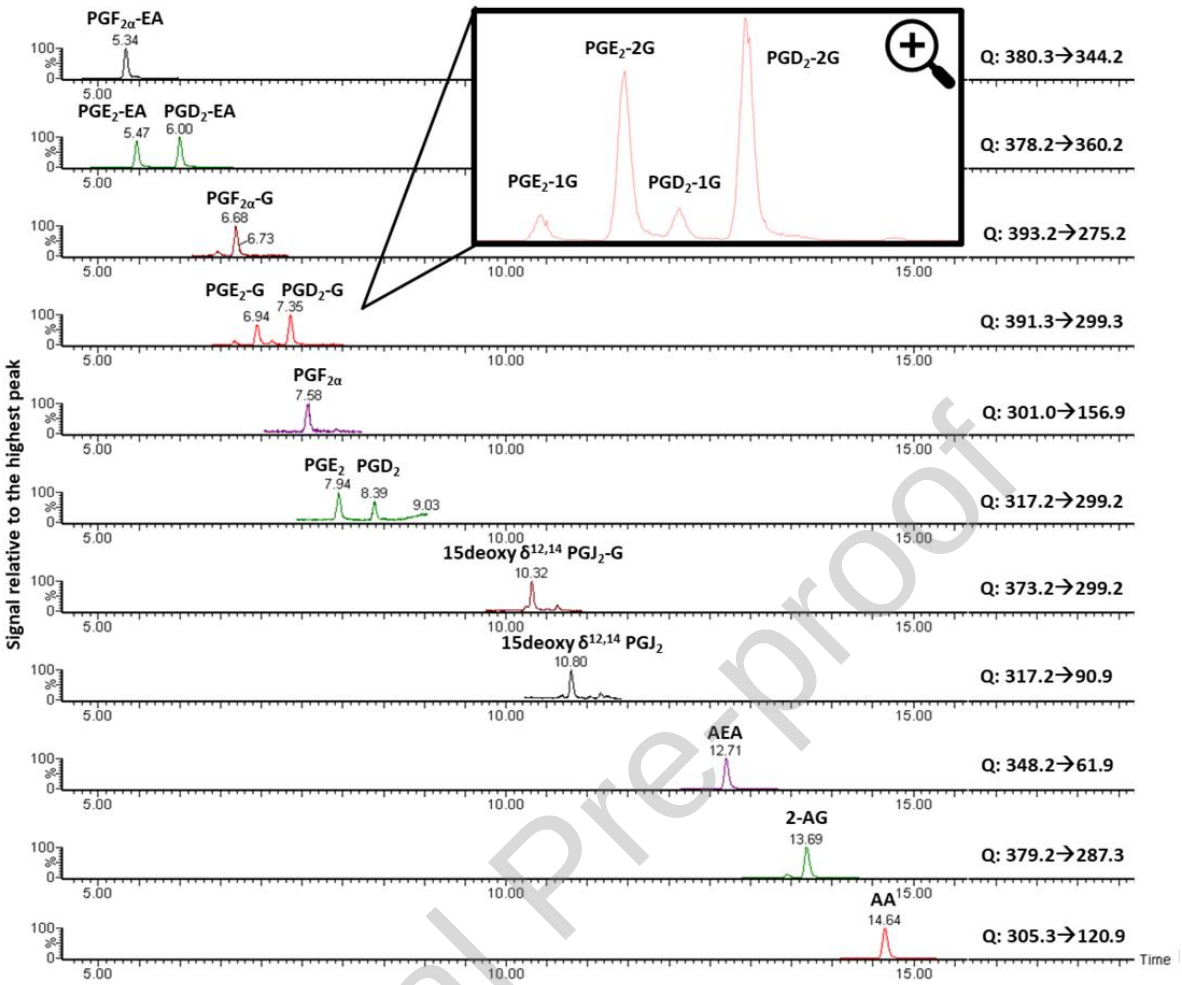

Figure 2: Typical chromatogram showing the analytical separation of the lipid mediators of interest. A mixture containing each standard (500 fmol) was injected on the UPLC-MS/MS system. For each standard, the signal corresponding to the quantitative transition is shown. The inset highlights the chromatographic separation between PGE_2-G and PGD_2-G as well as their respective position isomers (i.e. PGD_2-1-G, PGD_2-2-G, PGE_2-1-G and PGE_2-2-G).

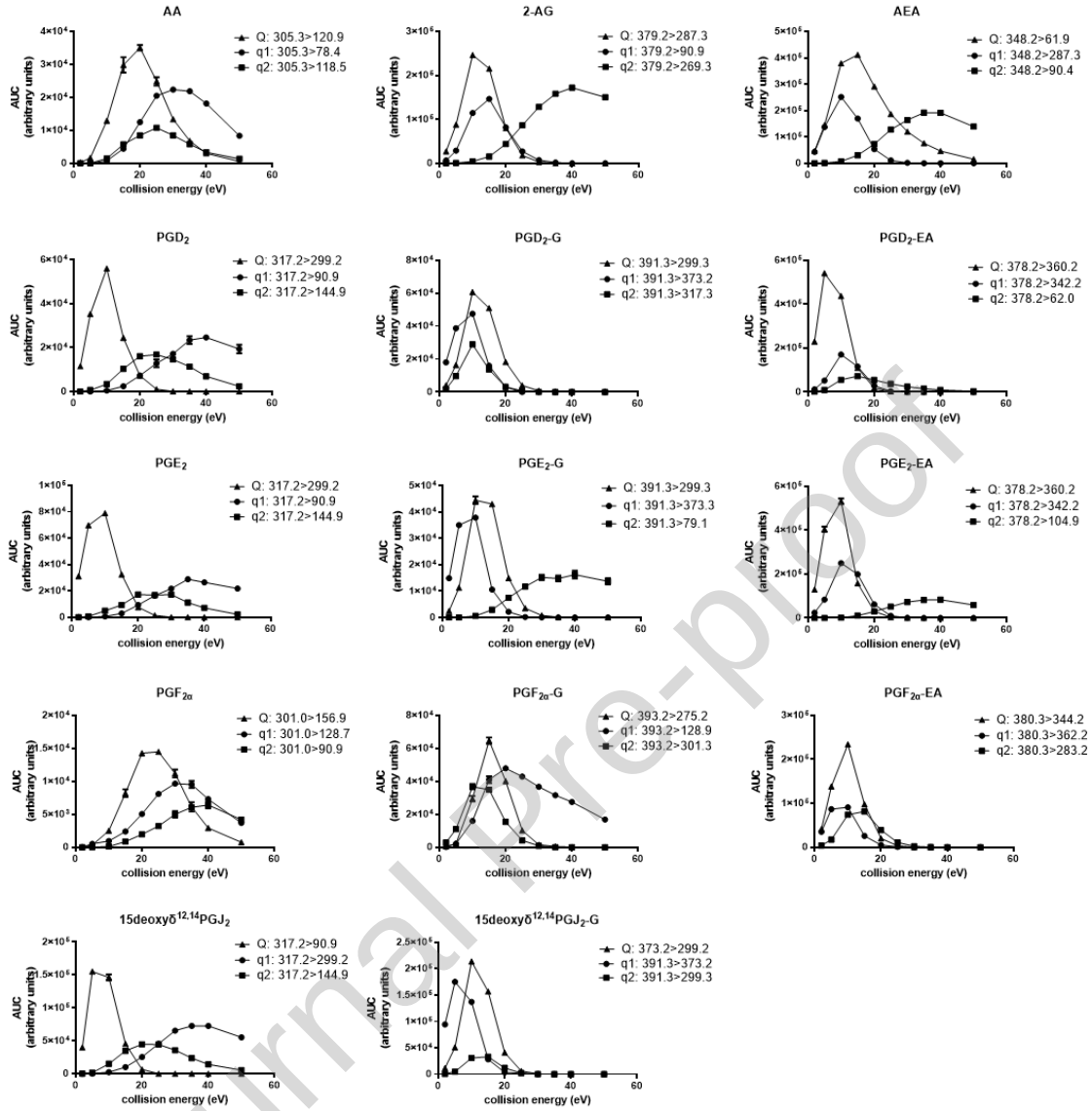

Figure 3: Determination of the MRM transition parameters. Standard solutions (500 fmol each analyte) were used for the set up. A fixed cone voltage of 30 V was used, while the effect of the collision energy of the three main MRM of each analyte was assessed between 2 eV and 50 eV. Signals (AUC) are plotted in function of the collision energy (eV) used. Q: quantitative transition, q1 and q2: qualitative transitions.

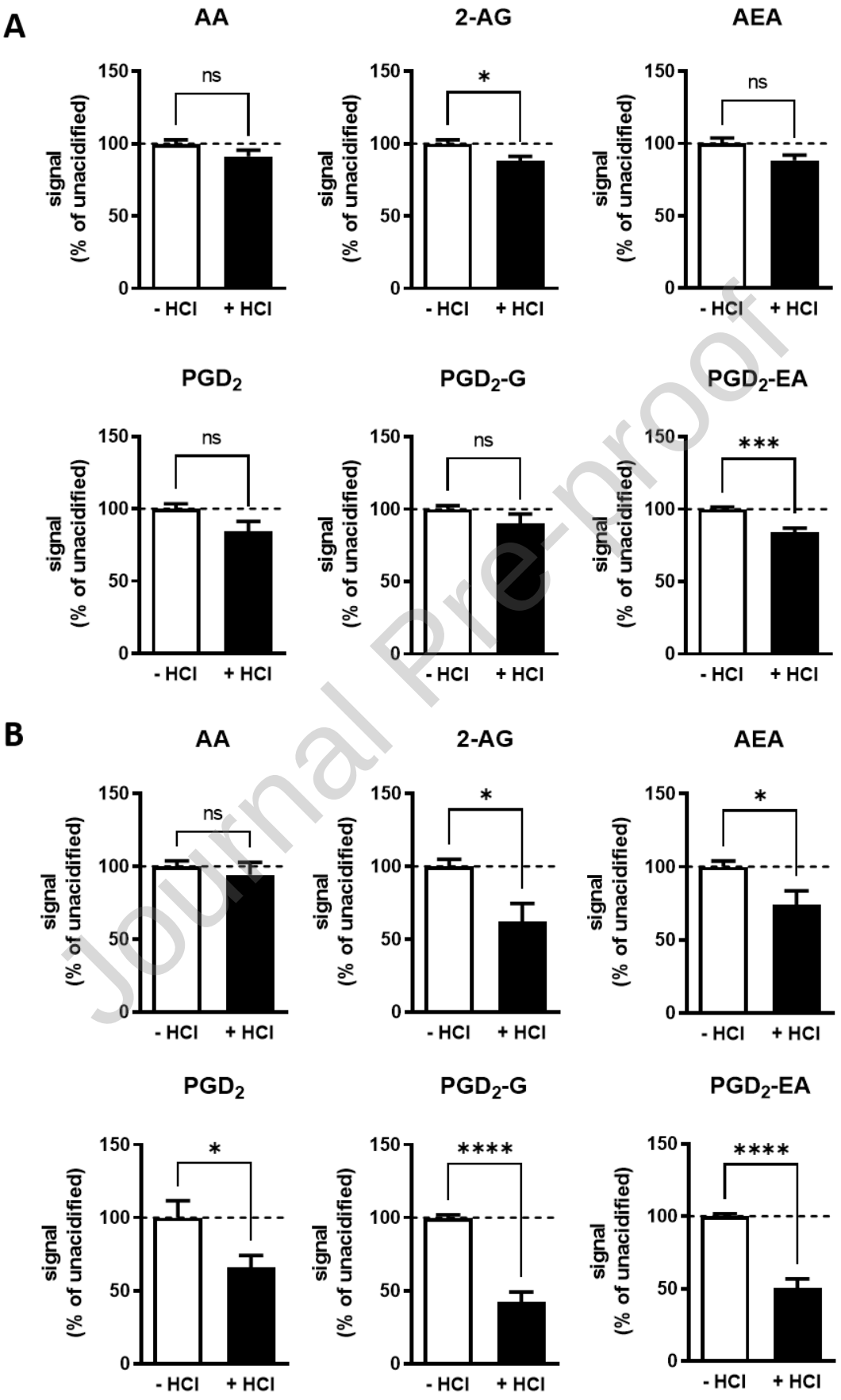

Figure 4: Assessment of the effect of the acidification during the extraction procedure. Six analytes (arachidonic acid, 2-AG, AEA, PGD_2, PGD_2-G, PGD_2-EA), selected as representatives of the entire analytes of interest, were chosen to set up the extraction procedure. The standards were extracted by liquid-liquid extraction in the absence (**A**) or presence (**B**) of matrix (10 mg of mouse brain). In each condition, the effect of the acidification (HCl 2N, 300µL) of the extraction mixture ($CHCl_3$-MeOH-H_2O, 8:4:2, v/v/v) was assessed. The data are reported as relative to the signal (AUC) obtained for the unacidified (- HCl) condition. After normality assessment, student t-test or Mann-Whitney non-parametric test was used. FDR assessment based on Benjamini-Hochberg method. Adjusted P values * p< 0,05; *** p< 0,001; **** p< 0,0001; N=3 in triplicate.

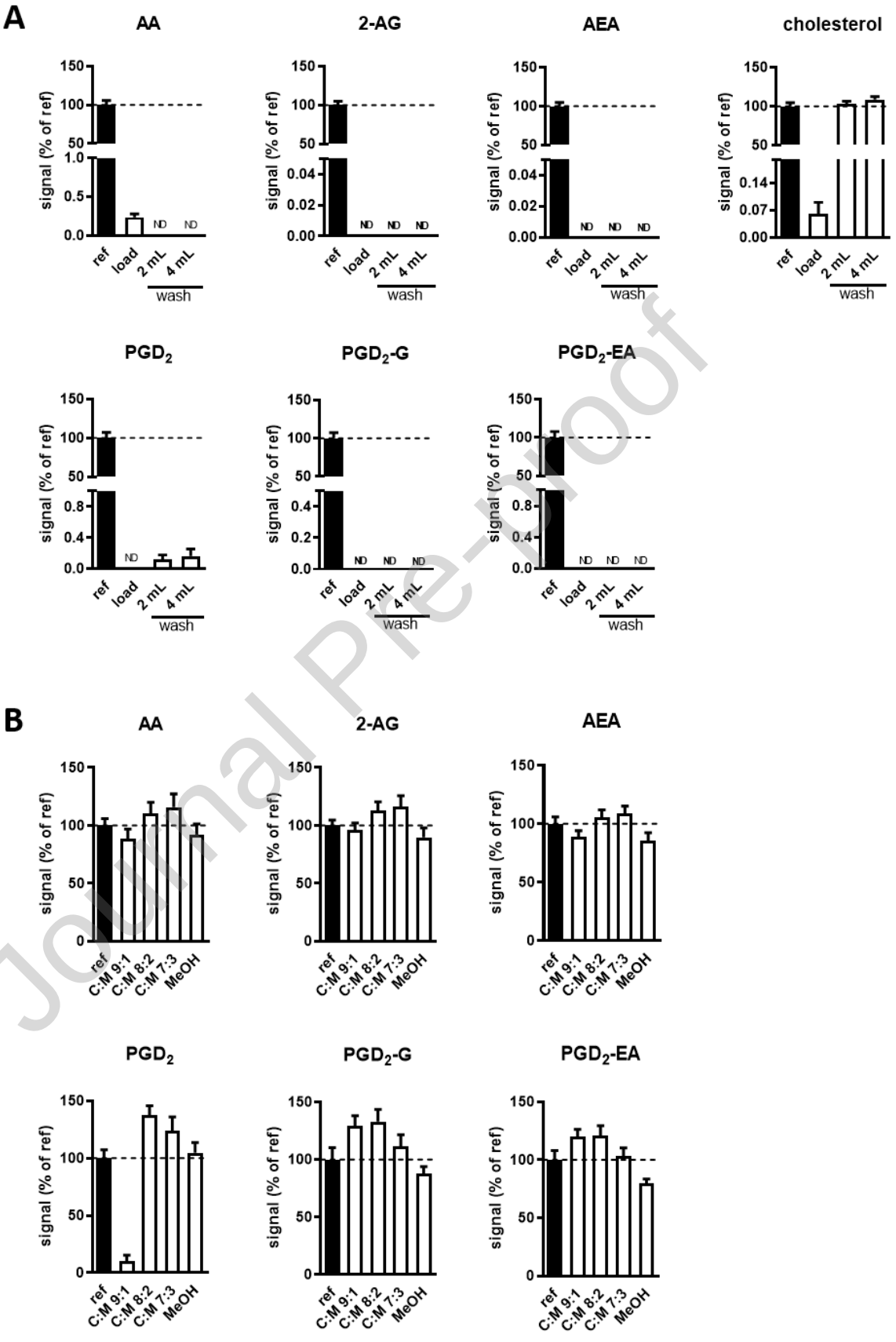

Figure 5: Optimization of the solid phase extraction procedure. Six analytes (arachidonic acid, 2-AG, AEA, PGD_2, PGD_2-G, PGD_2-EA), selected as representatives of the entire analytes of interest, were chosen to set up the SPE procedure. The standards were added to matrix (10 mg of mouse brain) before being extracted as reported above. (**A**) The lipid fractions were transferred on SPE silica columns using $CHCl_3$-MeOH (99:1; v/v). The flow through was recovered (load) as well as the eluting fractions obtained by using 2 mL or 4 mL of $CHCl_3$ as washing solvent. Following UPLC-MS/MS analysis, the data (AUC) are reported relative to the analysis of an extracted lipid fraction that did not went through the SPE procedure (ref). (**B**) To assess the elution of the analytes of interest, several mixtures of $CHCl_3$-MeOH were tested. The graph reports the data obtained following the elution using 3.5mL of $CHCl_3$-MeOH (9:1, v/v), $CHCl_3$-MeOH (8:2, v/v), $CHCl_3$-MeOH (7:3, v/v), or pure MeOH. Following UPLC-MS/MS analysis of the eluted fractions, the data (AUC) are reported relative to the analysis of an extracted lipid fraction that did not went through the SPE procedure (ref). N=3 in triplicate

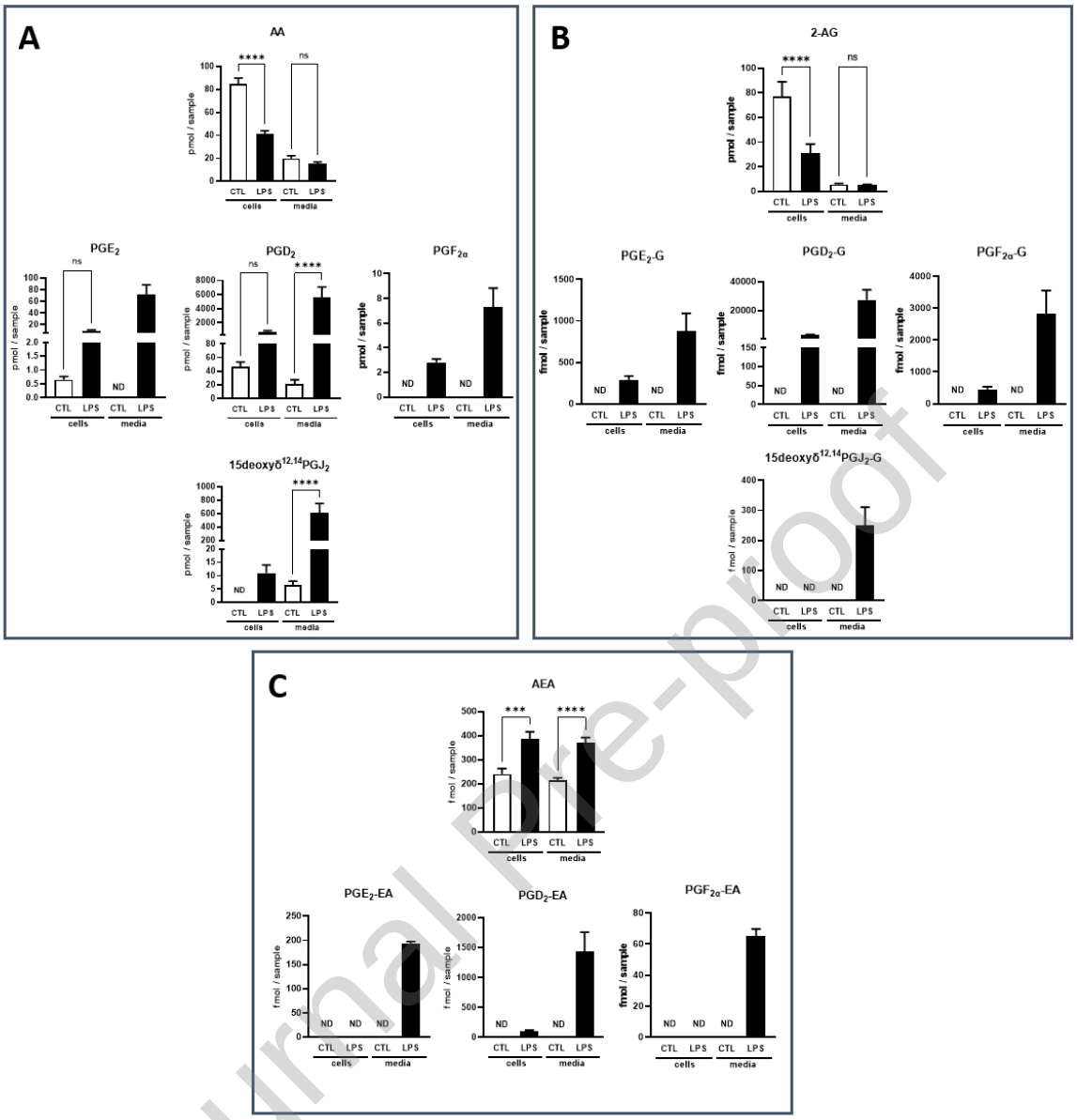

Figure 6: Quantification of the analytes of interest in J774 cells and their culture media following LPS activation. J774 cells were treated with vehicle (CTL) or with 100 ng/mL of LPS (LPS) for 24h. Then the cells and media were recovered and independently analyzed using the developed method. (**A**) Quantification of arachidonic acid and derived prostaglandins. (**B**) Quantification of 2-AG and derived prostaglandin-glycerol esters. (**C**) Quantification of anandamide and derived prostaglandin-ethanolamides. The signal (AUC) of each analyte was normalized with the AUC of the corresponding internal standard and the calibration curves used to convert the ratio into analyte levels (pmol or fmol per sample depending on the analyte). Data are expressed in mean ± SEM. N=3 in triplicate. After normality assessment, one-way Anova was used. *** p< 0,001; **** p< 0,0001 with Sidak's multiple comparison post-test.

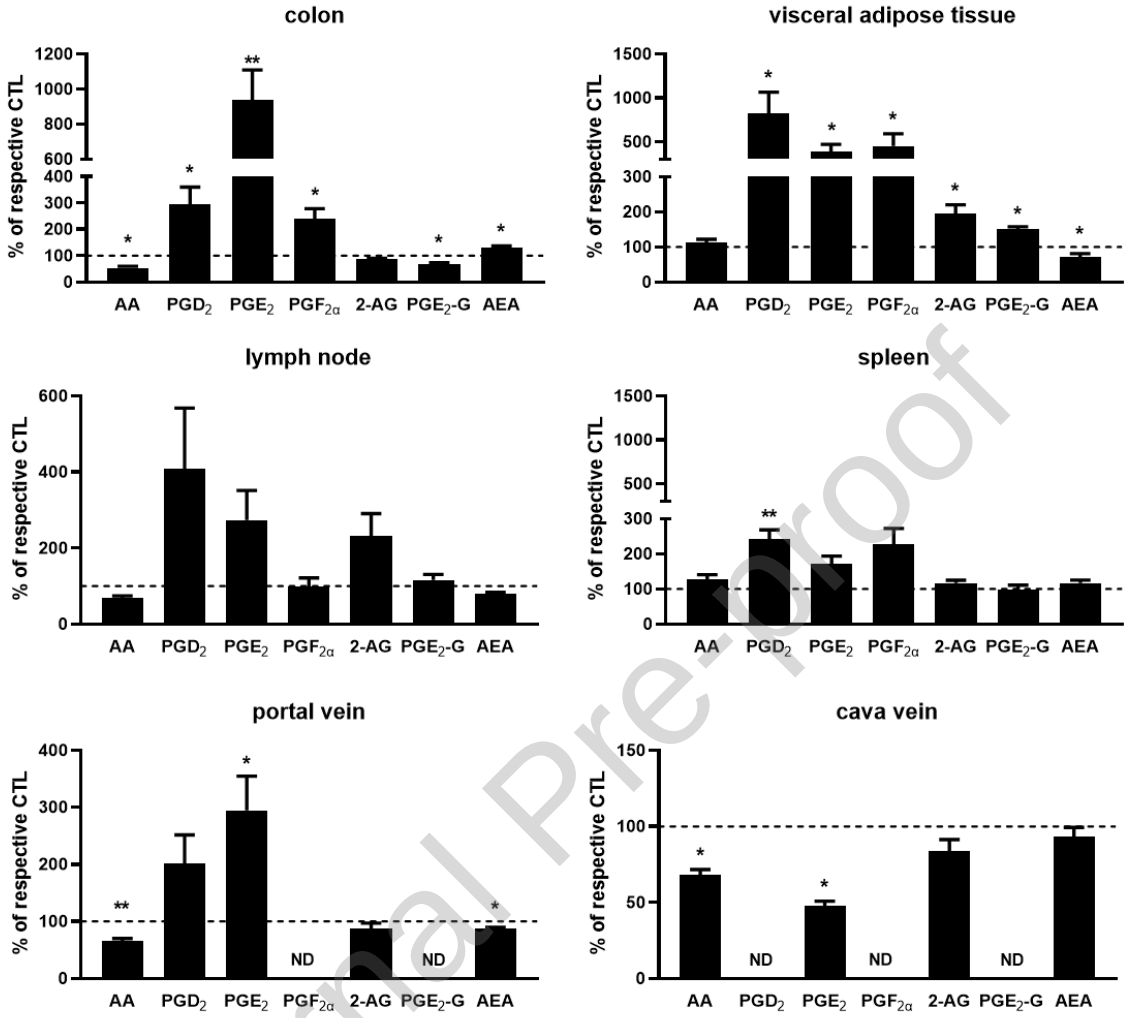

Figure 7: Quantification of the analytes of interest in DSS-induced colitis mice. Colitis was induced by adding DSS (5%) in the drinking water. Control mice (CTL) had access to drinking water throughout the study. On day 7, tissues (colon, lymphoid node, visceral adipose tissue, spleen, portal and cava vein plasma) were recovered. The levels of analytes were analyzed in each tissue and are reported here relative to the control group set at 100% (dotted line). Data are expressed in mean ± SEM (8 mice/group). The levels measured in both groups are reported in supplemental table 3. After normality assessment, student t-test or Mann-Whitney non-parametric test was used. FDR assessment based on Benjamini-Hochberg method. Adjusted P values * p< 0,05; ** p<0,01.

Table 1: Chemical and analytical description of the bioactive lipids of interest. Description of the fourteen molecules (and their respective internal standards) analyzed in the validated method. The table lists for each analyte the abbreviation used, molecular formula, molecular weight, analyzed ions, quantification (Q) and qualification (q) transitions as well as the relative retention time based on the respective internal standard. [a] molecular weight for the neutral form; [b] analyzed in positive mode; [c] quantitative (Q) and qualitative (q) transition used; [d] relative retention time (on the respective internal standard).

name	abbreviation	molecular formula	MW [a]	analyzed ion[b]	MRM transitions[c]	RRT[d]
arachidonic acid derivatives						
arachidonic acid	AA	$C_{20}H_{32}O_2$	304,5	$[M+H]^+$	Q: 305.3>120.9 q: 305.3>78.4	1.01
prostaglandin D_2	PGD_2	$C_{20}H_{32}O_5$	352,5	$[M+H-2H_2O]^+$	Q: 317.2>299.2 q: 317.2>90.86	1.06
prostaglandin E_2	PGE_2	$C_{20}H_{32}O_5$	352,5	$[M+H-2H_2O]^+$	Q: 317.2>299.2 q: 317.2>90.86	1.00
prostaglandin $F_{2\alpha}$	$PGF_{2\alpha}$	$C_{20}H_{34}O_5$	354,5	$[M+H-3H_2O]^+$	Q: 301.0>156.9 q: 301.0>128.7	0.95
15deoxy$\delta^{12,14}$prostaglandin J_2	15deoxy$\delta^{12,14}$PGJ $_2$	$C_{20}H_{28}O_3$	316,4	$[M+H]^+$	Q: 317.2>90.9 q: 317.2>299.2	1.39
2-arachidonoylglycerol derivatives						
2-arachidonoylglycerol	2-AG	$C_{23}H_{38}O_4$	378,6	$[M+H]^+$	Q: 379.2>287.3 q: 379.2>90.9	1.00
prostaglandin D_2 - glycerol ester	PGD_2-G	$C_{23}H_{38}O_7$	426,6	$[M+H-2H_2O]^+$	Q: 391.3>299.3 q: 391.3>373.2	1.07
prostaglandin E_2 - glycerol ester	PGE_2-G	$C_{23}H_{38}O_7$	426,6	$[M+H-2H_2O]^+$	Q: 391.3>299.3 q: 391.3>373.2	1.01

prostaglandin $F_{2\alpha}$ - glycerol ester	$PGF_{2\alpha}$-G	$C_{23}H_{40}O_7$	428,6	$[M+H-2H_2O]^+$	Q: 393.2>275.2 q: 393.2>128.9	0.96
15deoxy$\delta^{12,14}$prostaglandin J_2 - glycerol ester	15deoxy$\delta^{12,14}$PGJ$_2$-G	$C_{23}H_{34}O_5$	390,5	$[M+H-H_2O]^+$ and $[M+H]^+$	Q: 373.2>299.2 q: 391.3>373.2	1.52
anandamide derivatives						
anandamide	AEA	$C_{22}H_{37}NO_2$	347,5	$[M+H]^+$	Q: 348.2>61.9 q: 348.2>287.3	1.00
prostaglandin D_2 - ethanolamide	PGD_2-EA	$C_{22}H_{37}NO_5$	395,5	$[M+H-H_2O]^+$	Q: 378.2>360.2 q: 378.2>342.2	1.10
prostaglandin E_2 - ethanolamide	PGE_2-EA	$C_{22}H_{37}NO_5$	395,5	$[M+H-H_2O]^+$	Q: 378.2>360.2 q: 378.2>342.2	1.01
prostaglandin $F_{2\alpha}$ - ethanolamide	$PGF_{2\alpha}$-EA	$C_{22}H_{39}NO_5$	397,5	$[M+H-H_2O]^+$	Q: 380.3>344.2 q: 380.3>362.2	0.98
internal standards						
d_8-arachidonic acid	d_8-AA	$C_{20}H_{24}D_8O_2$	312,5	$[M+H]^+$	Q: 313.3>82.9 q: 313.3>111.0	/
d_5-1-arachidonoylglycerol	d_5-1-AG	$C_{23}H_{33}D_5O_4$	383,6	$[M+H]^+$	Q: 384.3>287.3 q: 384.3>269.3	/
d_4-anandamide	d_4-AEA	$C_{22}H_{33}D_4NO_2$	351,6	$[M+H]^+$	Q: 352.2>65.9 q: 352.2>287.3	/
d_4-prostaglandin E_2	d_4-PGE_2	$C_{20}H_{28}D_4O_5$	356,5	$[M+H-2H_2O]^+$	Q: 321.2>275.0 q: 321.2>148.9	/
d_5-prostaglandin E_2 - glycerol ester	d_5-PGE_2-G	$C_{23}H_{33}D_5O_7$	431,6	$[M+H-2H_2O]^+$	Q: 396.3>299.3 q: 396.3>79.1	/
d_4-prostaglandin E_2 - ethanolamide	d_4-PGE_2-EA	$C_{22}H_{33}D_4NO_5$	399,6	$[M+H-H_2O]^+$	Q: 382.2>364.3 q: 382.2>346.2	/

Table 2: Summary of the validation parameters obtained for each analyte of interest. The table summarizes the main validation parameters. The range of calibration curves, the equation of the curves, the limit of detection (LOD), the limit of quantification (LOQ), the repeatability, the intermediate precision, the accuracy and the linearity are listed for each molecule. The equations reported correspond to the equation of the linear regression obtained for the different calibration curves. The LOD and LOQ are reported in femtomole on column. Repeatability and intermediate precision: CV (%) values obtained for each analyte after the assessment of the four quality control levels within the same day or on three different days. Accuracy: bias (%) obtained considering the four quality control levels analyzed at three different time points. Linearity: slope and goodness of fit (R^2) of the linear regression line obtained when plotting the values (in femtomole) obtained for four different levels (quality control levels used in this case) with the theorical values used. [a-c] values expressed in femtomoles; [d] trueness (evaluated on the three calibration curve levels) expressed in relative bias (%); [e] intraday precision; [f] interday precision

analyte	range[a]	equation	LOD[b]	LOQ[c]	quality control level	trueness[d]	repeatability (% CV)[e]	intermediate precision (% CV)[f]	accuracy	linearity	
AA	400 - 9000	Y = 0,004586*X + 0,02251	100	400	LOQ		3,23	6,31	6,15	slope	0,99
					LOW	1,55	7,65	6,39	6,77		
					MIDDLE	-0,19	11,20	6,44	2,25	R^2	0,999
					HIGH	1,52	8,37	5,85	3,10		
PGD_2	100 - 900	Y = 0,004629*X - 0,1383	60	100	LOQ		8,29	8,89	4,17	slope	1,07
					LOW	-17,34	11,53	5,72	1,65		
					MIDDLE	-11,84	10,68	13,20	1,56	R^2	0,981
					HIGH	2,59	9,47	8,82	-2,50		
PGE_2	100 - 900	Y = 0,03153*X - 0,1345	60	100	LOQ		8,50	9,27	5,40	slope	1,01
					LOW	-4,46	10,78	6,35	4,44		
					MIDDLE	0,80	9,11	13,80	1,45	R^2	0,991
					HIGH	-8,01	7,22	8,17	-1,01		
$PGF_{2\alpha}$	200 - 900	Y = 0,006977*X - 0,1375	60	200	LOQ		9,32	8,19	5,58	slope	1,01
					LOW	-10,17	8,03	9,25	5,04		
					MIDDLE	-2,85	8,83	14,92	0,37	R^2	0,999
					HIGH	-0,25	9,14	11,05	1,48		
15deoxy$\delta^{12,14}$ PGJ_2	100 - 1800	Y = 0,05947*X - 1,316	50	100	LOQ		8,15	9,77	2,98	slope	1,04
					LOW	-3,97	10,71	6,93	3,46		
					MIDDLE	-2,98	8,84	13,19	-1,60	R^2	0,998
					HIGH	-2,57	9,40	9,68	-1,85		
2-AG	400 - 9000	Y = 0,0009628*X - 0,04477	10	60	LOQ		6,10	3,21	0,74	slope	0,98
					LOW	0,88	3,30	4,05	-0,58		

					MIDDLE	0,36	4,48	6,82	-2,01	R^2	0,999
					HIGH	0,89	4,92	6,90	-1,78		
PGD_2-G	100 - 900	Y = 0,0005303*X + 0,004200	40	100	LOQ		7,63	8,26	3,06	slope	0,99
					LOW	-11,01	7,87	9,04	1,12		
					MIDDLE	-3,82	6,14	10,14	-1,01	R^2	0,993
					HIGH	-4,94	6,77	10,04	-0,79		
PGE_2-G	50 - 900	Y = 0,001314*X - 0,02856	15	50	LOQ		2,17	8,91	2,58	slope	1,03
					LOW	-8,25	5,88	9,49	2,47		
					MIDDLE	-1,35	9,12	11,89	0,76	R^2	0,999
					HIGH	1,35	6,71	9,48	0,81		
$PGF_{2\alpha}$-G	40 - 900	Y = 0,001459*X - 0,01017	15	40	LOQ		9,14	4,71	5,45	slope	0,97
					LOW	0,64	6,82	5,33	2,56		
					MIDDLE	0,25	8,68	9,22	0,56	R^2	0,995
					HIGH	0,64	6,75	8,64	1,01		
15deoxy$\delta^{12,14}$ PGJ_2-G	100 - 900	Y = 0,002491*X + 0,005640	30	100	LOQ		6,93	6,74	-1,85	slope	1,02
					LOW	-4,74	5,94	9,99	-1,67		
					MIDDLE	-2,52	8,75	10,61	-3,40	R^2	0,993
					HIGH	1,96	8,60	8,23	-2,01		
AEA	40 - 900	Y = 0,009939*X - 0,03533	0,5	3	LOQ		11,45	16,57	0,26	slope	0,99
					LOW	1,81	4,51	5,62	-2,70		
					MIDDLE	-1,82	4,42	6,64	-3,10	R^2	0,999
					HIGH	0,12	5,36	8,17	-4,30		
PGD_2-EA	40 - 900	Y = 0,0001673*X + 0,0008319	10	30	LOQ		7,04	3,69	1,94	slope	1,01
					LOW	-3,87	6,33	6,25	2,64		
					MIDDLE	-0,90	8,88	9,91	-0,24	R^2	0,994
					HIGH	-3,21	7,76	8,11	-0,86		
PGE_2-EA	40 - 900	Y = 0,0005560*X - 0,01120	6	20	LOQ		8,73	6,34	2,28	slope	1,03
					LOW	-3,91	6,34	8,06	0,83		
					MIDDLE	-0,88	8,59	12,30	-2,06	R^2	0,996
					HIGH	1,41	6,33	7,77	-0,16		
$PGF_{2\alpha}$-EA	40 - 900	Y = 0,0002526*X - 0,001414	3	8	LOQ		7,69	14,19	15,32	slope	1,00
					LOW	2,01	6,10	6,94	1,40		
					MIDDLE	-0,87	7,78	10,28	-1,10	R^2	0,999
					HIGH	-0,50	7,14	8,56	-0,29		

Highlights

- Glycerol and ethanolamide analogues of prostaglandins are important lipid mediators
- They endogenous levels are low requiring sensitive analytical methods
- We developed and validated an UPLC-MS/MS method for their quantification from biological matrix

- DSS-induced colitis alters the levels of prostaglandins as well as their glycerol and ethanolamide analogues